Int. J. Multiphase Flow Vol. 17, No. 4, pp. 425–437, 1991
Printed in Great Britain.

0301-9322/91 $3.00 + 0.00

BUBBLE GROWTH ON A SOLID WALL IN A RAPIDLY-DEPRESSURIZING LIQUID POOL

Z. WANG† and S. G. BANKOFF‡
Chemical Engineering Department, Northwestern University, Evanston, IL 60208-3120, U.S.A.

(Received 10 July 1990; in revised form 1 January 1991)

Abstract—Experimental measurements were made of bubbles growing on a well-wetted stainless-steel surface in rapidly-depressurized distilled water. The Jones & Zuber variable-pressure solution for the bubble radius was modified by including the contribution of microlayer evaporation from the base of the bubble, as well as from the curved surface. Despite the pressure disturbances caused by acoustic reflections in the first few milliseconds, very good agreement is obtained with limited data.

Key Words: bubble growth, depressurization, microlayer

INTRODUCTION

The growth rate of a bubble on a solid wall in a rapidly-depressurizing liquid pool is of interest for many two-phase flow and heat transfer applications. For example, in a postulated loss-of-coolant accident in a pressurized-water reactor, or the rupture of a pressure-relief diaphragm in a runaway chemical reactor, the liquid, if initially subcooled, will depressurize to a saturated condition, and then begin to form vapor. The two-phase pool level, and thus eventually the discharge flow rate, are affected by the nucleation and growth rates of bubbles in the varying pressure field. In this paper we consider only bubble growth rates. A companion paper will report on bubble nucleation rates (Wang & Bankoff 1991). For rapid depressurization, with engineering surfaces in clean water, nearly all the initial bubbles are nucleated on the solid walls, rather than in the bulk liquid. In the first few milliseconds after a large vessel or diaphragm rupture, the pressure drops rapidly. Bubbles form on the walls, but have no time to coalesce, or rise due to buoyancy. The degree of non-equilibrium between the vapor in the bubbles and the bulk liquid determines the bubble growth rates. In the very earliest stage, growth is dominated by surface tension, but this effect becomes negligible before the bubble becomes visible to the naked eye. Nevertheless, this is a very slow growth period, resulting in a time delay between nucleation and significant bubble growth. The next stage is momentum-controlled, since little cooling of the liquid at the bubble wall has as yet taken place. Finally, the diffusion of heat through the thermal boundary around the bubble controls the bubble growth. For constant external pressure, it is then found that the bubble radius increases as the square root of time (Birkhoff *et al.* 1958; Scriven 1959; Bankoff 1963, 1966).

Bubble growth on solid walls under rapid depressurization presents additional complications, since the vapor density changes with time. Furthermore, a very thin liquid microlayer generally exists (if the wall is well-wetted) between the bubble and the wall. The evaporation of this microlayer contributes to the bubble growth. The work reported in this paper consists of an experimental and analytical approach to the problem. Bubble growth rates on a non-heated, vertical stainless-steel surface, under rapid depressurization, are measured by high-speed motion photography. A bubble growth equation, based on the Jones & Zuber (1978) solution for variable pressure, but taking into account the contact with the solid surface, is developed. The results should be useful in matching the early level swell period to the later quasi-equilibrium period, when the vapor and liquid temperatures are nearly equal, and the relative velocity of the vapor and liquid can be estimated by drift–flux correlations. These results may also be applicable to flashing

†Present address: Fauske & Associates, Burr Ridge, Ill., U.S.A.
‡To whom all correspondence should be addressed.

flow in converging nozzles. A liquid particle experiences rapid depressurization as it passes through the converging section. At some point nucleation and bubble growth begin, and temperature non-equilibrium between the liquid and vapor persists for a considerable distance downstream.

LITERATURE REVIEW

The problem of vapor bubble growth under constant external pressure is non-linear and cannot be solved exactly, except under simplifying assumptions which may be inherently contradictory. Thus, a similarity solution was discovered by Birkhoff *et al.* (1958), and also Scriven (1959), with the assumptions of (1) zero initial bubble radius and (2) no liquid inertia or surface tension. Hence the vapor is always at the saturation temperature at the given external pressure. The surface-tension-controlled and liquid-momentum-controlled phases of bubble growth are thus bypassed, only the late diffusion-controlled stage being considered.

Plesset & Zwick (1952, 1954) and Zwick & Plesset (1955) solved the problem of bubble growth in a superheated liquid from an initial slight displacement from equilibrium, all the way to late diffusion-controlled growth, by matched asymptotic expansions. The late-stage expansion parameter was the ratio of the volume of the thermal boundary layer around the bubble to the volume of the bubble. In order to deal with the moving boundary, the radial coordinate in the convective heat equation in the liquid was replaced by a Lagrangian coordinate. Since the liquid velocity at any point is related to the bubble wall velocity by the continuity equation, the solution for the temperature profile through the thermal boundary layer at the bubble wall, and hence for the bubble volume at any instant of time, immediately becomes implicit. Further, in order to allow an analytical solution of the zeroth-order heat flow problem, a time-like variable was introduced, which contained the bubble radius, and further ensured an indirect, parametric solution. For the late-stage growth, the zeroth-order error was bounded by solving the first-order problem, and bounding the resulting integral. To lowest order, the bubble radius increases as the square root of time, and the surface heat flux varies inversely as the square root of time. The solution is thus of the same form as the solution for a plane slab subjected to a step-change in surface temperature, except for a proportionality factor. This factor [called a sphericity factor, K_s, by Forster & Zuber (1954)] accounts for the stretching and thinning of the thermal boundary layer as the bubble surface area increases. For the Plesset–Zwick (P–Z) solution compared to the plane-slab solution, $K_s = \sqrt{3}$. Since the plane-slab solution for the surface flux, when a time-varying surface temperature is imposed, is well-known, this suggests that a good approximation to the bubble growth problem may be obtained by multiplying the corresponding plane-slab solution by the constant-surface-temperature sphericity factor. This was the approach adopted by Jones & Zuber (1978) for a bubble in a infinite sea of liquid in a decreasing-pressure field, and followed herein for a bubble attached to a solid with a non-zero contact angle, likewise in a decreasing-pressure field. It should be emphasized, however, that there is no rigorous basis for this approach. These authors used a sphericity factor $K_s = \pi/2$, derived by Forster & Zuber (1954) (F–Z) for the late-time growth of a bubble in an isothermal, constant-pressure liquid. However, the F–Z solution avoided the inherent non-linearity of this problem by modeling the growing bubble as a spherical heat sink, expanding through a stationary liquid at a rate dictated by mass and energy conservation. The stretching and thinning of the thermal boundary layer owing to convection is thus not present, leading to a growth rate about 10% slower than the P–Z solution. In this work we use the P–Z value, which also gives a better fit to our bubble growth data. Birkhoff *et al.* (1958) also obtain the value $K_s = \sqrt{3}$ as a limiting case of their similarity solution for fast-growing bubbles.

The P–Z solution was extended by Bankoff (1963) to third order, taking into account lower-order corrections resulting from simultaneously expanding the heat and liquid momentum equation. Skinner & Bankoff (1964, 1965) extended the P–Z procedure to spherically-symmetric initial temperature distributions in the liquid, and finally, to arbitrary initial temperature distributions.

Mikic *et al.* (1970) found a useful similarity solution for the dimensionless bubble radius, R^+, as a function of dimensionles time, t^+, by interpolating between the limiting cases of pure

momentum control and pure heat-conduction control of bubble growth at constant external pressure with uniform initial liquid temperature. This can be verified from their equation

$$R^+ = \tfrac{2}{3}[(t^+ + 1)^{1.5} - t^{+1.5} - 1] \qquad [1]$$

for small and large values of t^+. The analysis was also extended to bubble growth on a wall at constant contact angle. Unfortunately, there seems to be no simple way of extending their solutions to time-varying external pressures.

Theofanous *et al.* (1969) obtained a numerical solution for bubble growth in a time-dependent pressure field, assuming a quadratic temperature distribution across the thermal boundary layer. The effects of liquid viscosity, liquid inertia, surface tension, interfacial non-equilibrium and varying vapor density could all be included. Inoue & Aoki (1975), Cha & Henry (1981) and Toda & Kitamura (1983) examined the same problem by introducing a coordinate transformation which immobilized the moving boundary. Inoue & Aoki (1975) obtained the interfacial temperature in terms of a convolution integral involving the interfacial heat flux, and also presented an asymptotic solution for the bubble radius in a slowly-varying pressure field by an extension of the P–Z solution. Toda & Kitamura (1983) employed a thin thermal layer approximation, together with a similarity solution. The agreement between their predictions and their experimental data, obtained by a pulsed laser to form a bubble nucleus, was good when the sphericity factor $K_s = \pi/2$ was included.

Jones & Zuber (1978) solved the bubble growth problem in a variable pressure field by an extension of the F–Z method (1954), using the same value of K_s. For a linear decay with time of the bubble wall temperature, the solution obtained was

$$R(t^*) = \left(\frac{\rho_{v0}}{\rho_v}\right)^{1/3} R_0 \left\{1 + \frac{2K_s}{\sqrt{\pi}}\left[\mathrm{Ja_T} t^{*0.5} + \tfrac{2}{3}\mathrm{Ja_P} t^{*1.5}\right]\right\}, \qquad [2]$$

where t^* is a dimensionless time, given by $\alpha t/R_0^2$, $\mathrm{Ja_T}$ and $\mathrm{Ja_P}$ are Jakob numbers for initial superheat and for pressure effects, and ρ_{v0} and R_0 are the vapor density and bubble radius at the beginning of the thermally-controlled growth period.

Zwick (1960) solved the problem of the diffusion-controlled growth of a vapor bubble in a constant-pressure liquid with internal heat sources. This problem is equivalent to the decreasing pressure problem, with the exception that the vapor density remains constant. Zwick assumed a linear increase of liquid temperature with time. In this case the bubble radius grows initially as $t^{1/2}$, but for long times as $t^{3/2}$.

Tsung-Chang & Bankoff (1986) modified the Zwick solution to account for the system depressurization, and the consequent vapor density variation. Assuming that the relative rate of change of the vapor density is much smaller than that of bubble volume, a solution was obtained for the bubble radius vs time in parametric form. Numerical solutions were obtained, which were compared with the predictions of previous investigations. Burelbach & Bankoff (1987) performed a direct numerical integration of the integral equation expressing the energy balance on the bubble in Lagrangian coordinates, which agreed closely with the Tsung-Chang & Bankoff (1986) solution.

ANALYSIS

We consider the problem of a single vapor bubble growing on a vertical wall in an isothermal liquid pool subjected to sudden depressurization. Since the sound velocity in the vapor is large compared with the bubble wall velocity, the pressure within the vapor follows instantaneously its value at the bubble wall, which is given by the equilibrium vapor pressure of the liquid. Furthermore, the liquid can be taken to be incompressible. We assume also that temperature gradients within the bubble can be neglected, although for very fast-growing bubbles this assumption can lead to appreciable errors. For a discussion of these assumptions, see Plesset & Zwick (1954).

Significant complications are introduced by the attachment of the bubble to the solid wall. We assume that the bubble growing on the solid surface is always a truncated sphere, with contact angle, β, and that the center of the sphere is at rest with respect to the bulk liquid (figures 1a and 1b). These assumptions, which are made in order to make the problem tractable, are only approximately true. This is because the presence of the solid surface destroys the radial symmetry

of the liquid flow around the bubble. In particular, the contact angle depends upon the speed of the contact line close to the solid wall; there is a velocity boundary layer; there is a stagnation-point flow around the bubble owing to the translation of the bubble center toward the bulk liquid, and this, in turn, results in slight flattening of the bubble; and buoyancy may cause slight upwards translation of the bubble, although this was not observed in the time scale of these experiments.

In addition, it has been shown that a thin liquid microlayer exists at the base of a vapor bubble growing on a heated solid surface (Cooper & Lloyd 1969). It seems likely that this is true also for a bubble growing on an unheated wall (Katto & Shoji 1970). The estimation of the evaporative heat flux from the microlayer requires an integration over elements of surface area which have different times of appearance (Tsung-Chang & Bankoff 1989). The thickness of the microlayer, δ_{vis}, as a function of radial distance, r, was estimated by Cooper (1969) to be of the order of $(\nu t_b)^{1/2}$, where ν is the liquid kinematic viscosity, and $t_b(r)$ is the time when the bubble base radius was r.

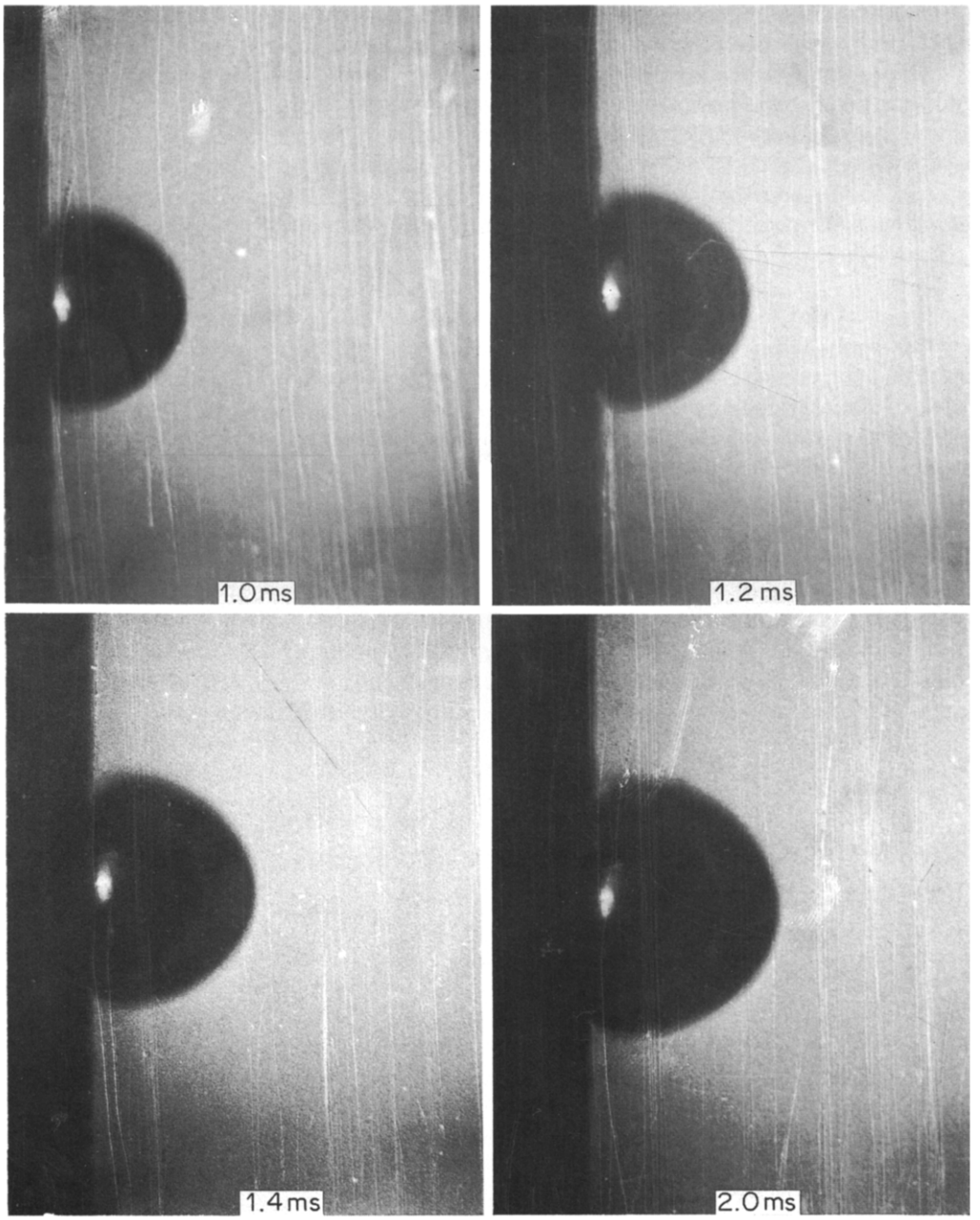

Figure 1a. Bubble shape and size in experiment 3010 (Table 1) at 2.0, 1.2, 1.4 and 2.0 ms after the bubble became visible. *Scale*: 0.0376 to 1.

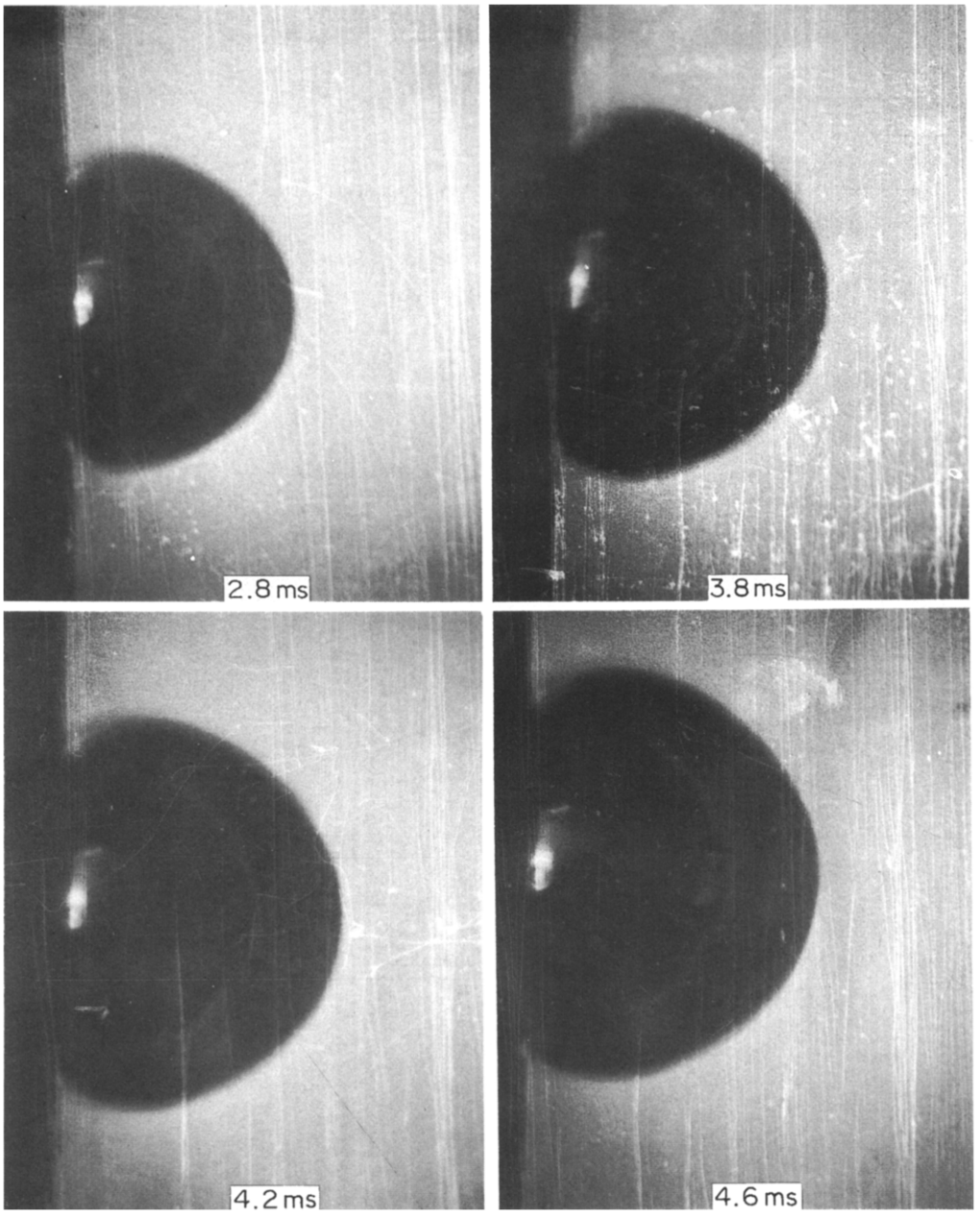

Figure 1b. Same bubble as in figure 1a, except at times 2.8, 3.8, 4.2 and 4.6 ms after the bubble became visible.

Once the surface element is exposed, evaporation begins and a thermal boundary layer, whose thickness, $\delta_{th}(r)$, is of the order of $[\alpha(t - t_b)]^{1/2}$, begins to penetrate into the liquid. For $\delta_{vis} \gg \delta_{th}$, the liquid layer can be assumed to be locally semi-infinite. For $t \leqslant 2t_b$, it is seen that $\delta_{vis}/\delta_{th} \leqslant \mathrm{Pr}^{-1/2}$, where Pr is the Prandtl number. Since $0 \leqslant t_b \leqslant t \leqslant t_f$, where t_f is the time of bubble observation, it is clear that this assumption is not valid for all t and r. Nevertheless, we follow Plesset & Prosperetti (1977) in assuming that the microlayer thickness is uniform at each time, and that the microlayer is exposed to the vapor for the same length of time as the curved portion of the bubble. Thus, the evaporative flux from the curved portion of the bubble is that from the flat microlayer, multiplied by the sphericity factor, K_s. Further discussion on microlayer heat transfer is given by Tsung-Chang & Bankoff (1989).

With these assumptions, the Rayleigh–Plesset equation in the liquid domain becomes

$$R\frac{\mathrm{d}^2R}{\mathrm{d}t^2} + \frac{3}{2}\left(\frac{\mathrm{d}R}{\mathrm{d}t}\right)^2 = \frac{1}{\rho_L}\left[P_v(t) - P(t) - \frac{2\sigma}{R}\right], \quad r > R(t), \quad 0 \leqslant \theta \leqslant \pi - \beta, \qquad [3]$$

where θ is the polar angle, taking the z-axis normal to the solid wall, and β is the apparent contact angle, assumed to be constant. The inertial terms on the l.h.s. are generally negligible by the time the bubble becomes visible to the naked eye, so that the bubble growth thereafter is thermally controlled. A criterion for this assumption to be valid is $\varepsilon \ll 1$, where

$$\varepsilon = \frac{P_0 - P_f}{\rho_L}\left(\frac{t_f}{R_f}\right)^2.$$

Here P_f, t_f and R_f are the final pressure, time after the initiation of bubble growth and the radius $R(t_f)$, respectively. From tables 1 and 2 it is found that ε is of the order of 10^{-1} for these bubbles. The neglect of the inertial terms is thus justified in this case, but it is seen that it might be necessary to consider the coupled momentum and heat transfer problem for rapid depressurization from much higher initial pressures. With these assumptions, the energy balance on the bubble separated from the solid by a very thin liquid layer is

$$\frac{d}{dt}(V\rho_v h_{fG}) = A_b\phi_b + A_c\phi_c, \qquad [4]$$

where ϕ_b and ϕ_c are the heat fluxes through the base and curved surface of the bubble, respectively. The bubble volume is

$$V(t) = \frac{\pi}{3}R^3(t)[2 + \cos\beta(2 + \sin^2\beta)], \qquad [5]$$

and the base area and curved surface area are, respectively,

$$A_b = \pi[R(t)\sin\beta]^2, \qquad [6]$$

and

$$A_c = 2\pi R^2(t)(1 + \cos\beta). \qquad [7]$$

In accordance with the previous discussion, we take

$$\phi_c = K_s\phi_b, \quad K_s = \sqrt{3} \quad \text{(Plesset \& Zwick 1954)}. \qquad [8]$$

Table 1. Experimental data for bubble 3010; $T_{f0} = 403$ K

Frame No.	t (ms)	P_∞ (bar)	R (mm)	D (mm)	H (mm)	β (deg)
1	0.20	1.72	0.58	1.11	0.74	73
2	0.40	1.70	1.03	1.95	1.28	74
3	0.60	1.67	1.30	2.49	1.67	73
4	0.80	1.65	1.57	3.0	1.99	74
5	1.00	1.63	1.70	3.23	2.24	71
6	1.20	1.60	1.88	3.55	2.49	71
7	1.40	1.58	2.00	3.78	2.67	70
8	1.60	1.56	2.10	3.98	2.77	71
9	1.80	1.54	2.17	4.1	2.88	71
10	2.00	1.52	2.30	4.33	3.06	70
11	2.20	1.50	2.42	4.55	3.23	70
12	2.40	1.48	2.54	4.76	3.41	70
13	2.60	1.46	2.66	5.01	3.54	70
14	2.80	1.45	2.79	5.27	3.7	71
15	3.00	1.43	2.89	5.43	3.91	69
16	3.20	1.41	2.95	5.57	3.93	70
17	3.40	1.39	3.01	5.68	4.02	70
18	3.60	1.38	3.13	5.90	4.18	70
19	3.80	1.37	3.22	6.09	4.26	71
20	4.00	1.36	3.28	6.2	4.36	70
21	4.20	1.36	3.38	6.4	4.48	71
22	4.40	1.36	3.48	6.57	4.64	70
23	4.60	1.36	3.55	6.68	4.73	70
24	4.80	1.36	3.64	6.84	4.87	70
25	5.00	1.35	3.71	6.98	4.97	70

Table 2. Experimental data for bubble 3101; $T_{f0} = 402$ K

Frame No.	t (ms)	P_∞ (bar)	R (mm)	D (mm)	H (mm)	β (deg)
1	0.20	1.74	0.30	0.5	0.46	57
2	0.40	1.71	0.39	0.64	0.62	54
3	0.60	1.70	0.51	0.90	0.77	61
4	0.80	1.71	0.56	0.99	0.81	63
5	1.00	1.73	0.67	1.20	0.95	65
6	1.20	1.76	0.69	1.25	1.0	64
7	1.40	1.78	0.77	1.39	1.09	65
8	1.60	1.80	0.79	1.43	1.11	66
9	1.80	1.78	0.86	1.57	1.2	66
10	2.00	1.76	0.92	1.67	1.30	65
11	2.20	1.73	1.01	1.85	1.44	65
12	2.40	1.67	1.04	1.90	1.48	65
13	2.60	1.61	1.17	2.13	1.68	65
14	2.80	1.55	1.26	2.31	1.76	67
15	3.00	1.49	1.35	2.45	1.90	66
16	3.20	1.43	1.45	2.69	1.99	68
17	3.40	1.38	1.55	2.87	2.13	68
18	3.60	1.33	1.65	3.10	2.22	70
19	3.80	1.39	1.79	3.37	2.41	70
20	4.00	1.25	1.94	3.55	2.71	69
21	4.20	1.22	2.00	3.74	2.73	69
22	4.40	1.22	2.01	3.74	2.73	69

From [6]–[8], the ratio of the heat flows from the base and curved portions of the bubble is given by

$$\varphi_1 \equiv \frac{A_b \phi_b}{A_c \phi_c} = \frac{\sin^2 \beta}{2\sqrt{3}(1 + \cos \beta)}. \quad [8a]$$

Taking $\beta = 70°$, $\varphi_1 = 0.19$, so that microlayer evaporation contributes a significant portion of the total heat transfer. Similarly, one can estimate the ratio of the heat transfer to the wall-attached bubble to that to an isolated bubble:

$$\varphi_2 \equiv \frac{\sin^2 \beta + 2\sqrt{3}(1 + \cos \beta)}{4\sqrt{3}}. \quad [8b]$$

For $\beta = 70°$, $\varphi_2 = 0.798$, so that the wall-attached bubble has a significantly slower vaporization rate. To obtain $R(t)$, one may use the parametric solution for the bubble radius given by Tsung-Chang & Bankoff (1986), or the modified plane-slab solution of Jones & Zuber (1978). The former solution has the advantage of not requiring arbitrary assumptions about the correction for convective thinning of the thermal boundary layer around the bubble, but is limited at present to a linear change in bubble wall temperature with time, which was not found in the present work. The modified procedure of Jones & Zuber (1978) was therefore adopted.

Even though the water layer beneath the bubble base is quite thin, it is acceptable to consider it to be a semi-infinite slab for the heat transfer times of interest (Plesset & Prosperetti 1977).

The surface heat flux of a semi-infinite slab, initially at a temperature T_0, which is subjected to a varying surface temperature $T(0, t) = T_0 - g(t)$, is given by Carslaw & Jaeger (1965):

$$\phi_b = \frac{k}{\sqrt{\pi \alpha}} \left[\frac{g(0)}{\sqrt{t}} + \int_0^t \frac{g'(\tau)}{\sqrt{t - \tau}} \, d\tau \right]. \quad [9]$$

Substituting [5]–[9] into [4] and integrating, one obtains

$$R = \left(\frac{\rho_{v0}}{\rho_v} \right)^{1/3} \left[R_0 + \frac{\Lambda}{h_{fg} \rho_{v0}} \int_0^t \left(\frac{\rho_{v0}}{\rho_v} \right)^{2/3} \phi_b(\tau) \, d\tau \right], \quad [10]$$

where the constant factor, $\Lambda = \Lambda(\beta, K_s)$, is

$$\Lambda = \frac{2K_s(1 + \cos \beta) + \sin^2 \beta}{2 + \cos \beta (2 + \sin^2 \beta)}. \quad [11]$$

From tables 1 and 2, it is seen that the apparent contact angle, β, is nearly constant over the time interval of interest, so that it is acceptable to take Λ out of the integral. We take the time, $t = 0$,

in [9] to be the time when significant bubble growth begins. Thus, $g(0)$ is the initial superheat for bubble growth, and $g'(t) > 0$ during the depressurization. The actual vapor densities, as calculated from the pressure measurements, were used in [10]. Even for this relatively small range of pressures, it is not acceptable to ignore this density correction inside the integral (Jones & Zuber 1978). A ninth-order polynomial was needed to fit the temperature–time curve calculated from the pressure–time data, since acoustic reflections caused large variations in pressure during the time interval of interest.

EXPERIMENT

The experimental vessel (figure 2) consisted of a vertical glass tube above which is mounted a measurement section. This was a 25.4 mm i.d. × 100 mm long stainless-steel tube, on which a sheathed thermocouple and two charge-type pressure transducers were mounted. Above the measurement section was a 3.8 cm i.d. stainless-steel cross, with a flange welded on each end. A pneumatic cylinder connected to a stainless-steel cutter was mounted horizontally on one flange. Depressurization was realized by nearly-instantaneous rupture of the 0.127 mm thick, 38 mm dia aluminum diaphragm, mounted on the flange opposite the cutter blade. A satisfactory diaphragm burst was almost always achieved, as shown by the rupture of the diaphragm into four nearly-identical quadrants. The top flange was blocked by a blind flange with its inner surface cut into a conical shape of 18° from the horizontal, so that the shock wave was not directly reflected back into the test vessel.

The test section was a 25.4 mm i.d. × 250 mm long glass tube, with a 3 mm thick wall and a hemispherical bottom. In order to avoid optical distortion in the measurement of the bubble dimensions, the glass tube had a 100 mm long flat surface. A silicone oil bath with magnetic stirrer was used to heat the test section.

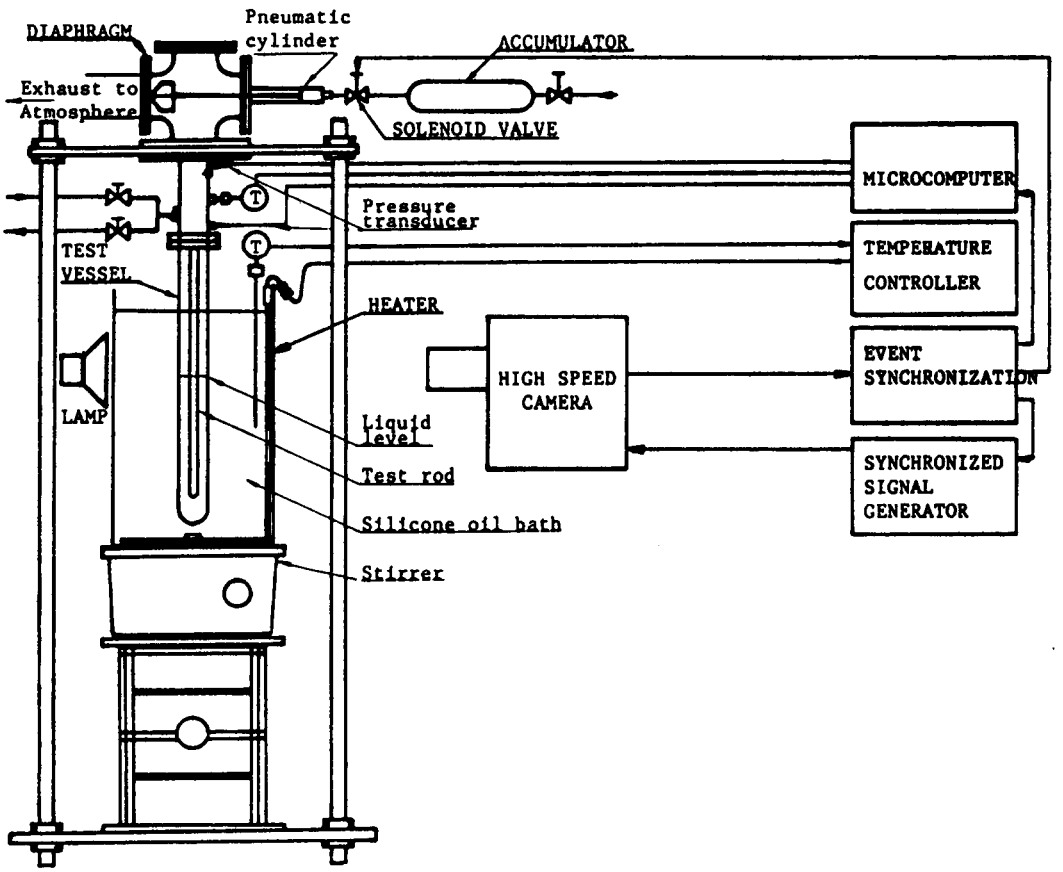

Figure 2. Diagrammatic sketch of the experimental apparatus.

A Photek-IV camera was used to take pictures of either the growing bubbles or the liquid level, at framing rates of 5000/s. A 1 kW high-intensity projection lamp was installed at the rear of the test section about 0.2 m away from the tube center. 100-ft rolls of Kodak Tri-X reversal black-and-white film were used for the experiment, and later developed using a Kramer Mark I processor in the laboratory.

After the film ran through a preset 40-ft length and was accelerated to the desired speed, an event control signal was generated by the camera, which simultaneously triggered the solenoid valve, a signal generator and the computer to begin data acquisition. The pulse from the signal generator activated an internal LED in the camera, producing an initialization mark on one side of the film. The camera itself also produced a 1 kHz timing mark on the other side of the film, which enabled the time for each frame of film and the corresponding pressure, to be determined.

The transient system pressure was measured by two charge-type, high temperature, high-sensitivity pressure transducers with a response time of 2 μs and an estimated error of $\pm$ 10^3 Pa. To measure the shock wave speed in the gas, the two transducers were installed 76 mm apart, with water-cooled jackets. The output from the transducers was converted to a voltage signal by a pressure transducer amplifier. The voltage was digitized and stored on a floppy disk. The pressure data file was later transferred to the main-frame computer. The pressure transducers were factory-calibrated, but were recalibrated frequently within $\pm 1\%$ by discharging nitrogen gas at known pressure from the test section into the atmosphere. Limited adjustments of the pressure transducer amplifier gain coefficient could be made. Factory recalibration was performed when necessary.

A sheathed chromel–alumel thermocouple was used to measure the system temperature. Because the response time of 5 ms of a 0.013 mm dia unsheathed thermocouple (the smallest commercially available) was of the same order of magnitude as the depressurization time, only the steady-state temperature was measured.

The objective was to measure bubble growth rates on a vertical stainless-steel rod with a milled flat surface. Deionized and distilled water was used as the test liquid. The test vessel was washed with soap several times, soaked in chromic acid cleaning solution for a day and then flushed with distilled water. Before being installed in the test section, the rod was also washed with soap, put into chromic-acid cleaning solution for 1 h and then washed with distilled water. It was attached to a thin stainless-steel bar, clamped between the test vessel and the measurement section. The water in the test vessel was allowed to boil for 10–20 min in order to degas the system. The vent valve was then closed, and the 16 mm high-speed camera was focused carefully on the center of the test surface. An $f = 100$ mm lens with a 50 mm extension tube was used to take pictures of single bubble

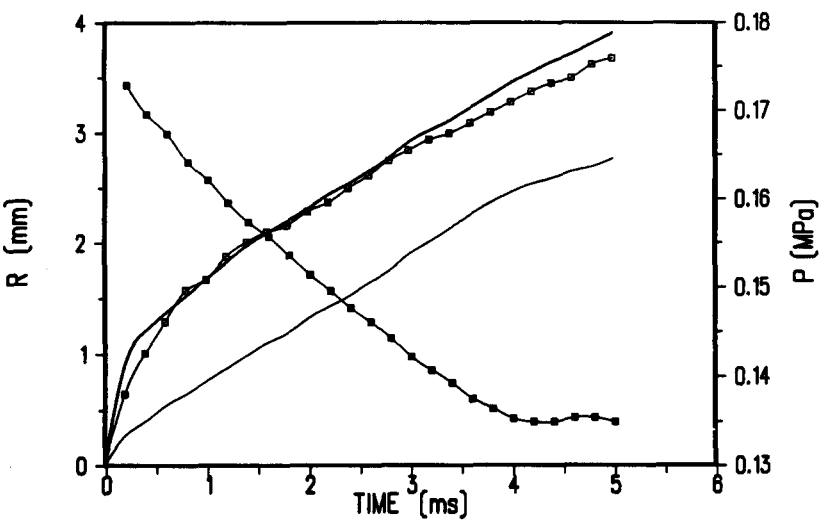

Figure 3. Radius–time measurements of bubble 3010 (table 1) compared with the modified Jones–Zuber (1978) analysis [9]–[11] and Mikic *et al.* (1970) constant-pressure solution. [1]; $T_{f0} = 402$ K. □, R (experiment); ——, R [10]; ——, R (Mikic *et al.* 1970); ■, P.

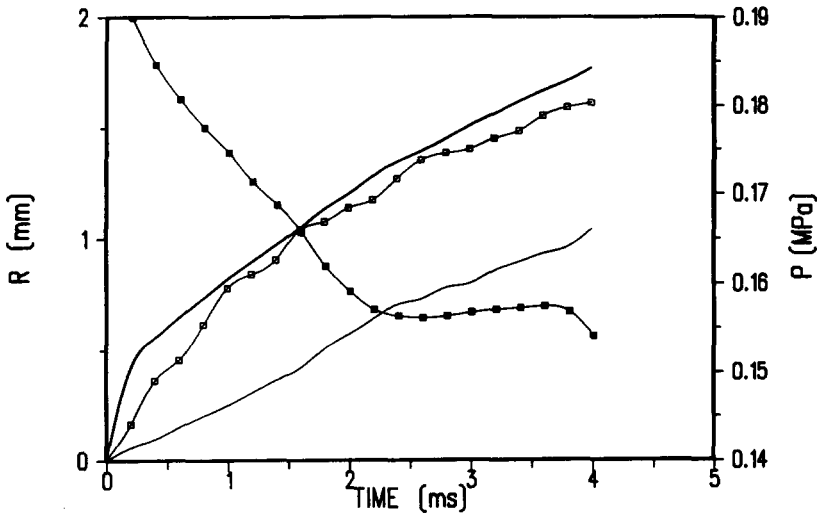

Figure 4. Same as figure 3, except for bubble 3161; $T_{f0} = 409$ K (Wang 1989). □, R (experiment); ——, R [10]; ——, R (Mikic *et al.* 1970); ■, P.

growth, and a +4 close-up lens was put on the $f/2.8$ lens to photograph a column of bubbles. The test rod diameter, or, in some cases, the distance between two artificial holes on the test rod surface, was used as the reference scale.

After the desired temperature (160°C) was reached, the oil bath was removed and the system was further pressurized by admitting nitrogen into the system. After switching on the pressure transducer amplifiers and the projection lights, the camera was started. After developing the film, the bubble diameters and heights were measured by projecting the image onto a screen. The estimated error was ± 0.01 mm.

RESULTS AND DISCUSSION

After considerable preliminary calibration, about five rolls of 100-ft film were successfully taken for bubble growth measurements. Tables 1 and 2 list measurements for typical bubbles. Other bubble measurements are tabulated in Wang (1989). The bubble shape, in general, is very nearly a truncated sphere with a fairly constant apparent contact angle, β, in the range 60°–75°. The equivalent-volume truncated-sphere bubble radius, R, is tabulated along with the measured base

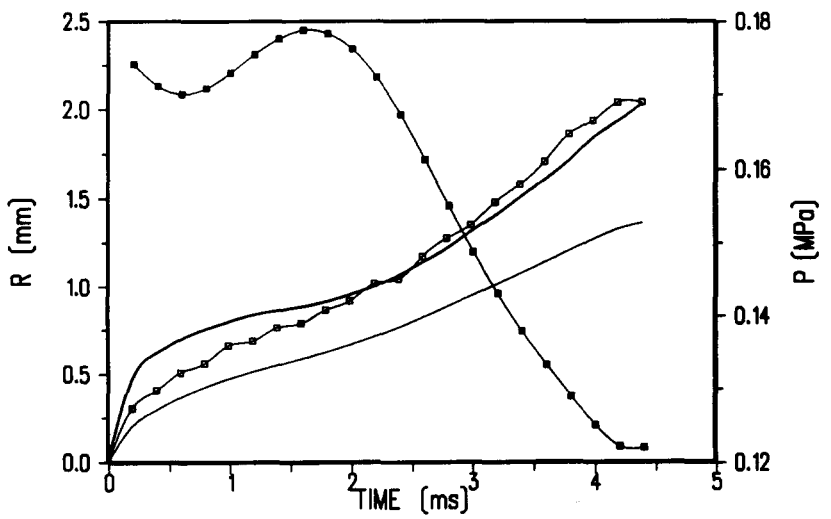

Figure 5. Same as figure 3, except for bubble 3101; (table 2); $T_{f0} = 402$ K. □, R (experiment); ——, R [10]; ——, R (Mikic *et al.* 1970); ■, P.

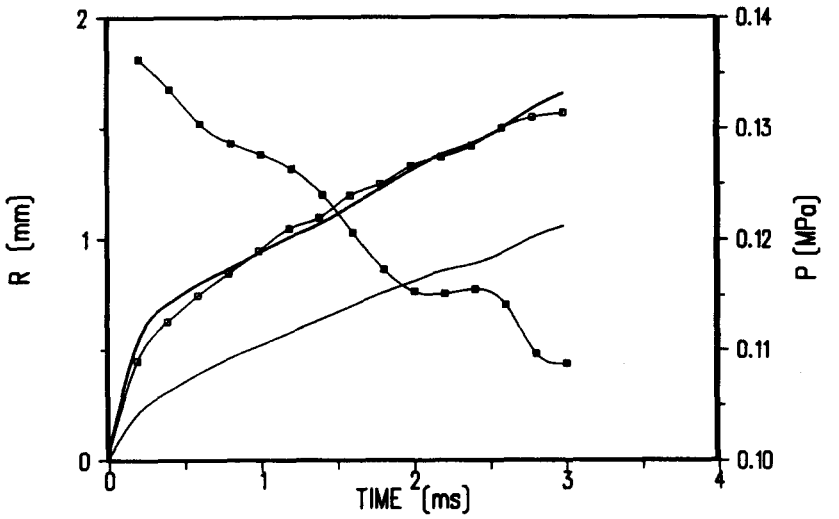

Figure 6. Same as figure 3, except for bubble 3171; $T_{f0} = 401$ K (Wang 1989). □, R (experiment); ——, R [10]; ——, R (Mikic *et al.* 1970); ■, P.

diameter, D, and height, H, of the growing bubble. The stainless-steel surface is, in fact, well-wetted by the water. Hence the apparent contact angle is an artifact of the microlayer deposition process, since the water cannot be immediately displaced at the solid surface by the vapor. No bubbles were found in the bulk liquid or on the glass walls during the depressurization time period. It can be concluded that for these relatively low liquid temperatures and with the existence of partially-wetted surfaces, heterogeneous nucleation at the test surface, rather than homogeneous nucleation, dominates the boiling process.

Bubble radii calculated from [9]–[11], are plotted in figures 3–7. Note the wide variations with time in system pressure, owing to acoustic reflections, and from bubble to bubble. Nevertheless, the predicted and measured radius–time curves are in agreement, within experimental error, with *no* adjustable constants. As expected, [1], since it was derived for constant vapor density and liquid superheat at the initiation of visible bubble growth, underestimates the bubble growth rate. It is again rather remarkable that the constant-pressure and variable-pressure curves are of similar shape, so that the displacement of the curves gives a measure of the effect of depressurization on increasing the bubble growth rate. Also, as shown by these figures, inertial effects, which slow down bubble growth, do not seem to be significant, since the predicted curves, which are based on purely

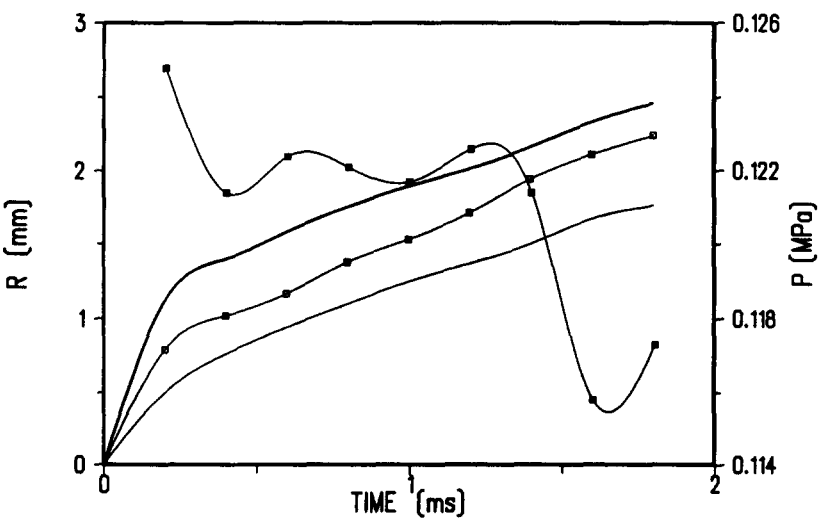

Figure 7. Same as figure 3, except for bubble 3103; $T_{f0} = 402$ K (Wang 1989). □, R (experiment); ——, R [10]; ——, R (Mikic *et al.* 1970); ■, P.

thermally-controlled bubble growth, are in good agreement with the measured growth curves. This good agreement also provides important, albeit indirect, evidence for the importance of microlayer evaporation in bubble growth from solid surfaces.

We show elsewhere (Wang & Bankoff 1991) that these results can be used to convert measurements of the rate of rise of the liquid level in the first few milliseconds to rates of effective bubble nucleation as function of time. Conversely, once the rates of effective bubble nucleation and growth are known in a rapidly-depressurizing vessel, one can estimate the rate of increase of average void fraction, and hence the rate of liquid level rise for very early times, while the bubbles are still attached to the walls. Once this period is over, as evidenced by bubble breakthrough from the free surface in the vessel, it is reasonable to assume that vapor–liquid equilibrium has been established. Hence drift–flux methods (Grolmes 1983) can be used to estimate the subsequent rate of level rise and vapor flow away from the free surface. It is hoped that the same concepts would apply to flashing flows through nozzles and pipe breaks.

Acknowledgement—Work supported by the National Science Foundation under Grant MEA-8212483.

REFERENCES

BANKOFF, S. G. 1963 Asymptotic growth of a bubble in a liquid with uniform initial superheat. *Appl. sci. Res.* **12,** 267–318.

BANKOFF, S. G. 1966 Diffusion-controlled bubble growth. *Adv. chem. Engng* **6,** 1–60.

BIRKHOFF, G., MARGULIES, R. S. & HORNING, W. A. 1958 Spherical bubble growth. *Phys. Fluids* **1,** 201–204.

BURELBACH, J. P. & BANKOFF, S. G. 1987 Vapor bubble growth under decompression conditions. *Physicochem. Hydrodynam.* **9,** 15–22.

CARSLAW, H. S. & JAEGER, J. C. 1965 *Conduction of Heat in Solids*, 2nd edn. OUP, Oxford.

CHA Y. S. & HENRY, R. E. 1981 Bubble growth during decompression of a liquid. *J. Heat Transfer* **103,** 56–60.

COOPER, M. G. & LLOYD, A. J. P. 1969 The microlayer in nucleate pool boiling. *Int. J. Heat Mass Transfer* **12,** 895–913.

FORSTER, H. K. & ZUBER, N. 1954 Growth of a vapor bubble in a superheated liquid. *J. appl. Phys.* **25,** 474–478.

GROLMES, M. A. 1983 A simple approach to transient two-phase level swell. In *Proc. of Condensed Papers from the 3rd Multiphase Flow and Heat Transfer Symp.*, Miami Beach, Fla, pp. 301–303.

INOUE, A. & AOKI, S. 1975 On the dynamics of bubble growth under time dependent pressure field. *Bull. Tokyo Inst. Technol.* **127,** 25–43.

JONES, O. C. JR & ZUBER, N. J. 1978 Bubble growth in variable pressure field. *J. Heat Transfer* **100,** 453–459.

KATTO, Y. & SHOJI, M. 1970 Principal mechanism of micro-liquid-layer formation on a solid surface with a growing bubble in nucleate boiling. *Int. J. Heat Mass Transfer* **13,** 1299–1311.

MIKIC, B. B., ROHSENOW, W. M. & GRIFFITH, P. 1970 On bubble growth rates. *Int. J. Heat Mass Transfer* **13,** 657–666.

PLESSET, M. S. & PROSPERETTI, A. 1977 Bubble dynamics and cavitation. *A. Rev. Fluid Mech.* **9,** 145–185.

PLESSET, M. S. & ZWICK, S. A. 1952 A nonsteady heat diffusion problem with spherical symmetry. *J. appl. Phys.* **23,** 95–98.

PLESSET, M. S. & ZWICK, S. A. 1954 The growth of bubbles in superheated liquid. *J. appl. Phys.* **5,** 493–500.

SCRIVEN, L. E. 1959 On the dynamics of phase growth. *Chem. Engng Sci.* **10,** 1–13.

SKINNER, L. A. & BANKOFF, S. G. 1964 Dynamics of vapor bubbles in spherically symmetric temperature field of general variation. *Phys. Fluids* **7,** 1–6.

SKINNER, L. A. & BANKOFF, S. G. 1965 Dynamics of vapor bubbles in binary liquids with spherically symmetric condition. *Phys. Fluids* **8,** 1417–1420.

THEOFANOUS, T. G., BIASI, L., FAUSKE, H. K. & ISBIN, H. S. 1969 A theoretical study on bubble growth in constant and time-dependent pressure fields. *Chem. Engng Sci.* **24,** 885–897.

TODA, S. & KITAMURA, M. 1983 Bubble growth in decompression fields. *Proc. ASME–JSME therm. Engng Joint Conf.* **3,** 395–402.

TSUNG-CHANG, G. & BANKOFF, S. G. 1986 Growth of a vapor bubble under flashing conditions. In *Proc. 8th Int. Heat Transfer Conference, San Francisco, Calif.* Hemisphere, New York.

TSUNG-CHANG, G. & BANKOFF, S. G. 1989 On the mechanism of forced-convection subcooled nucleate boiling. *J. Heat Transfer* **112,** 213–218.

WANG, Z. 1989 Ph.D. Thesis, Chemical Engineering Dept, Northwestern Univ., Evanston, Ill.

WANG, Z. & BANKOFF, S. G. 1991 Effective bubble nucleation rates on a solid wall in a rapidly-depressurizing liquid pool. In *Proc. 3rd ASME–JSME Joint therm. Engng Conf.*, Reno, Nev., Vol. 2, pp. 229–234.

ZWICK, S. A. 1960 Growth of vapor bubble in a rapidly heated liquid. *Phys. Fluids* **3,** 685–692.

ZWICK, S. A. & PLESSET, M. S. 1955 On the dynamics of small vapor bubbles in liquids. *J. Math. Phys.* **33,** 308–330.